arXiv:1406.3560v1 [physics.atom-ph] 13 Jun 2014

Doubly magic trapping for Cs atom hyperfine clock transitions

A. W. Carr and M. Saffman
Department of Physics, 1150 University Avenue,
University of Wisconsin, Madison, Wisconsin 53706
(Dated: June 16, 2014)

We analyze doubly magic trapping of Cs hyperfine transitions including previously neglected contributions from the ground state hyperpolarizability and the interaction of the laser light and a static magnetic field. Extensive numerical searches do not reveal any doubly magic trapping conditions for any pair of hyperfine states. However, including the hyperpolarizability reveals light intensity insensitive traps for a wide range of wavelengths at specific intensities. We then investigate the possibility of using bichromatic trapping light fields. Deploying a bichromatic scheme, we demonstrate doubly magic red and blue detuned traps for pairs of states separated by one or two single photon transitions.

PACS numbers: 37.10.Jk, 06.30.Ft, 37.10.Gh

The international primary standard for time is the Cs atom ground state hyperfine clock transition $|3,0\rangle \leftrightarrow |4,0\rangle$ which is defined to have a frequency of 9192631770 Hz. Coherent control of alkali atom clock states is of great interest for precision measurements[1] and for encoding neutral atom qubits for quantum computation experiments[2]. Although the clock states have excellent coherence properties in a field free environment, fluctuations of optical and magnetic trapping and bias fields lead to differential shifts of the clock state energies causing decoherence.

A large amount of recent work has been devoted to finding magic trapping conditions for which variations of external fields do not lead to a differential shift of the clock state energies. For alkali atom hyperfine transitions there are magic conditions for hyperfine Zeeman states with $M_F \neq 0$[3–6] which eliminate sensitivity to fluctuations of the trapping light but are still sensitive to magnetic noise. There are also magic conditions for states with $M_F = 0$ which are insensitive to light fluctuations at the cost of increased sensitivity to magnetic noise due to the requirement of a relatively large magnetic bias field of several Gauss[7–9]. In [10, 11] doubly magic traps were proposed which use $M_F \neq 0$ states with elliptically polarized light to cancel the sensitivity to fluctuations of both light and magnetic fields. These doubly magic conditions were restricted to certain wavelength ranges and required very precise preparation of the field polarization state.

In this letter we study magic trapping conditions while consistently accounting for the hyperpolarizability, which is fourth order in the electric field amplitude, as well as the interaction of the vector polarizability with the static magnetic field. As we illustrate in Fig. 1 and explain below these terms are important for accurate calculations of the differential shift (DS) at typical experimental trap depths. Including these effects, which were not fully accounted for in previous calculations, and after an extensive parameter search we find no parameters

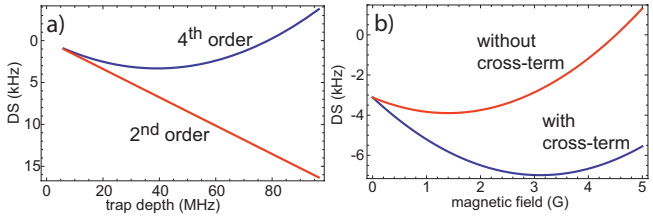

FIG. 1. (color online) Differential shift (DS) as a function of trapping light intensity and magnetic field. a) DS at $B = 0$ using 2nd order perturbation theory (red) and 4th order (blue) for the Cs clock states $|3,0\rangle, |4,0\rangle$ at $\lambda = 780$ nm. Notice the minimum in the DS as a function of the light intensity (trap depth) which constitutes a magic operating point. b) DS as a function of the magnetic field with (blue) and without (red) the third order cross-term for $\lambda = 780$ nm, $\Omega_0/2\pi = 100$ GHz, σ_+ polarization, and the states $|4,1\rangle, |3,-1\rangle$.

for doubly magic trapping in a monochromatic trapping light field. This suggests that previously reported doubly magic solutions[10] are not doubly magic. However, we demonstrate insensitivity to differential light shifts with only one frequency and pure circular polarization at specific intensities for a wide range of wavelengths.

Although we have not found doubly magic conditions with monochromatic trapping light, a bichromatic approach, following the proposal in [12], does allow for doubly magic trapping for red or blue detuned optical traps. Our results significantly extend the range of configurations which can be used for doubly magic trapping. In particular, we can make the the $M_F = 0$ clock transition $|4,0\rangle \leftrightarrow |3,0\rangle$ and the two photon transition $|4,1\rangle \leftrightarrow |3,-1\rangle$ doubly magic. Our solutions provide a viable and flexible approach for achieving extended coherence with trapped alkali atoms.

The calculational approach we follow is to use fine structure energies at zeroth order and treat the hyperfine and Zeeman interactions as perturbations. We use exact diagonalization to consistently include the fourth order hyperpolarizability, third order hyperfine-mediated

polarizability, and third order cross-term between the polarizability and the Zeeman interaction. An example of a Hamiltonian between Cs $6s_{1/2}$ $|F, M_F\rangle$ hyperfine states $|0\rangle = |3,1\rangle$ and $|1\rangle = |4,1\rangle$ is given in Eq. (1). Though these states are not ideal for magic conditions, for the case of non-elliptically polarized light their analysis reduces to a simple 2×2 matrix which serves to elucidate our procedure for searching for doubly magic traps. For states with different M_F values or elliptically polarized light the Hamiltonian can be constructed using the methods detailed in the supplementary material[13].

Our model Hamiltonian for these states is

$$\mathcal{H} = \begin{pmatrix} V_{\mathrm{hf},0} + V_{00} + \beta_{00} + Z_{00} & V_{01} + \beta_{01} + Z_{01} \\ V_{01} + \beta_{01} + Z_{01} & V_{\mathrm{hf},1} + V_{11} + \beta_{11} + Z_{11} \end{pmatrix}. \tag{1}$$

Here $V_{\mathrm{hf},i}$ is the diagonal hyperfine interaction, V_{ij} arises from the quadratic polarizability due to the trapping light, β_{ij} is from the third order diagonal and off-diagonal hyperfine-mediated polarizability, Z_{ij} is the magnetic dipole coupling due to the external magnetic field, and Z_{ii} are the first order diagonal Zeeman shifts. For all calculations we include the $6p_{1/2}, 6p_{3/2}, 7p_{1/2}, 7p_{3/2}$ levels, excited $ns_{1/2}$ states up to $14s_{1/2}$ and the counter-rotating terms. Mathematical details on how to compute these terms are in the supplementary material[13]. To check our results we compare against experimental data in [5] for the differential light shift per unit of intensity. For 780 nm light they record $-2.27(40) \times 10^{-2}\,\mathrm{Hz/W/cm^2}$ compared to our value of $-2.02 \times 10^{-2}\,\mathrm{Hz/W/cm^2}$ and for 532 nm light they measured $-3.51(70) \times 10^{-4}\,\mathrm{Hz/W/cm^2}$ whereas we calculate $-4.08 \times 10^{-4}\,\mathrm{Hz/W/cm^2}$. Thus, in both cases we are within experimental error bars and differ by no more than 15%.

The eigenvalues of (1), replacing the diagonals by $\Delta E_0, \Delta E_1$, are

$$\delta E_{1,0} = (\Delta E_0 + \Delta E_1 \pm \sqrt{4(V_{01} + Z_{01})^2 + (\Delta E_1 - \Delta E_0)^2})/2$$

where we ignore β_{01} for the moment since $V_{01} \gg \beta_{01}$. In the limit where the hyperfine interaction dominates other perturbations, i.e. $(\Delta E_1 - \Delta E_0)^2 \gg (V_{01} + Z_{01})^2$, the differential shift relative to the hyperfine splitting $V_{\mathrm{hf},1} - V_{\mathrm{hf},0}$ is

$$\delta E = \beta_{11} - \beta_{00} + Z_{11} - Z_{00} + 2\frac{Z_{01}^2 + 2V_{01}Z_{01} + V_{01}^2}{\Delta E_1 - \Delta E_0}. \tag{2}$$

$V_{00} = V_{11}$ since the electric dipole operator only couples to the electronic quantum numbers which are the same for both states and thus they cancel out of the differential shift. From here we can make the connection to non-degenerate perturbation theory. The last three terms, from left to right, are: the second order Zeeman shift, the third order cross-term that is two electric dipole matrix elements and one magnetic dipole coupling matrix element and finally a hyperpolarizability term which is fourth order in the electric dipole operator. Figure 2 depicts the physical origin of the higher order terms.

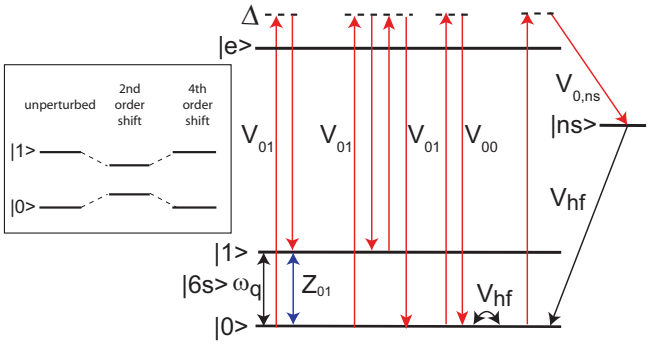

FIG. 2. (color online) Schematic representation of four of the terms important to calculating the differential shift where V_{ij} indicates the polarizability between states i and j. From left to right we have the cross-term of two electric dipole couplings and a magnetic dipole coupling. This can also happen in reverse order thus the extra factor of two in Eq. (2). Next is the fourth order term with four electric dipole couplings. This is also the crucial term in the bichromatic scheme except that it then couples to the other ground state that is dressed by a sideband energy very close to the qubit splitting. Third, we have the hyperfine-mediated polarizability term that is diagonal in the ground state hyperfine interaction (HFI). Last is the hyperfine-mediated polarizability term involving HFI-induced mixing of the ground $6s_{1/2}$ state and excited ns states.

Now we can write down a system of equations that need to be solved for doubly magic conditions to exist. We make the following replacements in order to isolate the dependence on the amplitude of the optical trapping field $\mathcal{E}$ and the magnetic field B: $\Omega_0 = \frac{\mathcal{E}}{\hbar}\langle 6p_{1/2}||er||6s_{1/2}\rangle$, $\beta_{11} - \beta_{00} \to \beta^{(1)}\Omega_0^2$, $Z_{11} - Z_{00} \to \mu^{(1)}B$, $2\frac{Z_{01}^2}{\Delta E_1 - \Delta E_0} \to \mu^{(2)}B^2$, $4\frac{V_{10}Z_{01}}{\Delta E_1 - \Delta E_0} \to \beta^{(2)}\Omega_0^2 B$, $2\frac{V_{01}^2}{\Delta E_1 - \Delta E_0} \to \beta^{(4)}\Omega_0^4$. Then the differential shift is

$$\delta E = \mu^{(1)}B + \mu^{(2)}B^2 + \beta^{(1)}\Omega_0^2 + \beta^{(2)}\Omega_0^4 + \beta^{(4)}\Omega_0^2 B$$

and after taking the appropriate derivatives

$$\frac{d\delta E}{dB} = \mu^{(1)} + 2\mu^{(2)}B + \beta^{(2)}\Omega_0^2, \tag{3}$$

$$\frac{d\delta E}{d\Omega_0^2} = \beta^{(1)} + \beta^{(2)}B + 2\beta^{(4)}\Omega_0^2. \tag{4}$$

Doubly magic trapping occurs when both derivatives simultaneously vanish for a set of parameters (Ω_0, B), thus eliminating the first order sensitivity to both electric and magnetic fields.

It is the implications of the cross-term with coefficient $\beta^{(2)}$, and $\beta^{(4)}$ the hyperpolarizability, that drive the novel results in this paper. The cross-term has been partially included before in [10] where doubly magic wavelengths were calculated by determining the magic magnetic field

TABLE I. Intensity magic trap conditions for various wavelengths, light polarizations, pairs of states, and magnetic fields. Also reported are the first order sensitivities to the magnetic field, and the second order sensitivities to the reduced Rabi frequency. The polarization is either σ_+ or σ_- and the states column lists $m_{F=4}, m_{F=3}$. Finally, trap depth for blue detuned traps refers to the light shift the atom experiences at the bottom of the trap rather than the actual depth of the trap. The ground state scalar polarizability is negative for the 780 and 820 nm cases so the trap depths are positive, i.e. repulsive potentials.

λ (nm)	σ	states	B (G)	$\Omega_0/2\pi$ (GHz)	trap depth (MHz)	$\frac{d\delta E}{dB}$ (Hz/G)	$\frac{d^2\delta E}{d\Omega_0^2}$ (10^{-18}Hz^{-1})
1038	+	0,0	1.4	158.0	-60.0	-2440	2.50
1038	+	0,0	1.0	150.0	-54.3	-2440	2.26
1038	+	0,0	0	129.0	-40.3	-2440	1.60
1038	+	1,-1	1.4	164	-66.5	-3680	2.53
945	+	-1,1	1.4	70.8	-23.3	-1000	10.4
820	+	0,0	1.4	70.4	35.5	-3680	22.4
780	+	0,0	1.4	124	49.2	-2720	4.68
780	-	1,-1	1.4	85.6	24.3	1760	2.10

with no light interacting with the atoms, i.e. ignoring the last term in Eq. (3). However, this neglects the fact that through this term the light intensity also affects the magic magnetic field value, that is, we have a coupled system of equations. In addition the effects of the fourth order term at the end of Eq. (4) have not previously been accounted for. As we will show, this term cannot be neglected and the implication is that there exist not magic wavelengths, but magic intensities for most wavelengths. Finally, we emphasize that while solving the above equations will yield approximately correct results, our primary search method is to diagonalize the ground state Hamiltonian and look for local minima (or maxima) in the differential shift that is equivalent to a doubly magic operating point.

The influence of the hyperpolarizability on magic trapping conditions has been shown to be important for optical atomic clocks[14], but has been neglected in previous analyses of microwave clocks. When field strengths reach 10^8 V/m the hyperpolarizability cannot be neglected when calculating energy shifts of alkali atom ground states[15]. To put this value in perspective an optical dipole trap for Cs atoms based on a modest power of 20 mW at $\lambda = 1.06$ μm focused to a waist ($1/e^2$ intensity radius) of $w = 2$ μm gives a field strength $> 10^6$ V/m and a trap depth of 15.5 MHz. For detunings large compared to the excited state hyperfine structure we can estimate when the contribution of the fourth order term to the differential shift becomes as important as that of the hyperfine-mediated polarizability, i.e. the magic intensity point. $\beta^{(1)} \sim -\omega_q\Omega_0^2/\Delta^2$ and $\beta^{(4)} \sim \Omega_0^4/(\omega_q\Delta^2)$, with ω_q the hyperfine splitting of the two states and Δ the detuning from the excited state, which suggests an order of magnitude of $P_{magic} \sim \Omega_0^2 \simeq \omega_q^2$. The implications of this relationship are that the hyperpolarizability becomes important at lower intensities in atomic species with smaller ground state hyperfine splitting, e.g. Rubidium compared to Cesium. Fig. 1 illustrates the importance of the fourth order and cross-terms by graphing the differential shift with and without them.

The primary lesson to be drawn from these two terms is that it is inappropriate to talk about magic wavelengths. Even if searching purely for magic conditions in one field the operating laser intensity and magnetic fields are interdependent and the system is now nonlinear in the intensity. Adjusting the laser intensity then tunes the relative strength of these terms and allows for magic conditions at a more diverse set of wavelengths.

Unfortunately we were unable to find doubly magic conditions for monochromatic trapping light of any wavelength for any pair of states. It is possible that some elliptical polarization we did not check or just a more precise calculation could turn up something useful. What we can say is that for most wavelengths, magnetic field strengths, pairs of states and polarizations there is a magic intensity where first-order sensitivity to the light intensity is zero. Table I provides examples of magic intensities for various atomic and field parameters, as well as the residual field sensitivities. As one can see, despite not being truly doubly magic, the sensitivity to the magnetic field can be quite small for some magic intensity conditions, in particular at 945 nm with the unorthodox $|4,-1\rangle$ and $|3,1\rangle$ states. If one can stabilize the magnetic field to 100 μG then the above states can have differential shifts of about 0.1 Hz.

It is worth pointing out some of the trends in Table I. Increasing the bias magnetic field increases the trap depth of the magic intensity for the states $0,0$. Similarly, increasing the detuning increases the trap depth and decreases the residual sensitivity to the trapping light. We chose 1.4 G for the magnetic field since it is very close to the magic magnetic field for the $M_F = 0$ states with no trapping light and thus elucidates how important a proper accounting of the aforementioned cross-term is for accurately assessing magic conditions.

In order to achieve true doubly magic traps we adopt

TABLE II. Doubly magic conditions for red and blue detuned traps for different wavelengths, pairs of states, sideband strengths (ratio of sideband field amplitude to carrier field amplitude), sideband frequency, and the residual sensitivities to field fluctuations.

λ (nm)	states	SB strength	$\omega_s/2\pi$ (GHz)	B (G)	$\Omega_0/2\pi$ (GHz)	trap depth (MHz)	$\frac{d^2\delta E}{dB^2}$ ($\frac{\text{Hz}}{\text{G}^2}$)	$\frac{d^2\delta E}{d\Omega_0^2}$ (10^{-18}Hz^{-1})
1038	0,0	0.1	9.15	1.35	88.3	-19	854	2.49
1038	0,0	1	8	1.39	63.6	-19.5	854	4.97
1038	1,-1	1	8	3.63	80.7	-32.2	801	7.5
1038	-1,1	0.1	9	1.78	135	-43.5	801	2.59
920	0,0	0.1	9.185	0.364	17.7	2.26	854	18.5
920	0,0	0.1	9.15	1.54	27.2	-5.89	854	34.6
780	0,0	0.1	9.185	0.27	29.9	2.89	854	3.56
780	0,0	0.1	9.17	0.798	51.4	8.56	854	4.1

the idea of Radnaev et al.[12]. They envisioned applying another laser that would couple the two ground $6s$ hyperfine levels via a two-photon transition where the photon fields differ in frequency by very near the hyperfine splitting of the two ground states. Practically, this could be accomplished by a high frequency phase modulator that adds a frequency shifted sideband at approximately the hyperfine ground splitting, e.g. $\omega_\text{s} \sim \omega_\text{q} = 9.192$ GHz in Cesium. Thus, we obviate the need for another laser and automatically match the intensity profile of the second light frequency to that of the primary trapping light.

We modify our computational apparatus to incorporate dressed ground states that differ by plus or minus a sideband frequency. Essentially, the Hamiltonian matrix grows three fold as for each ground state we add two levels with identical quantum numbers to the original except that the diagonal element has $\pm\omega_s$, the difference between the carrier and sideband frequencies. The matrix is then populated as before. We include an explicit example in [13]. A fourth order term that is roughly $V_{ij}^s V_{ij}^s/(\omega_q - \omega_s)$ arises, where V_{ij}^s uses the field amplitude of the sideband and the carrier, i.e. $\Omega_0^2 \to \Omega_0\Omega_s$ with Ω_s the reduced Rabi frequency of the sideband. This term is much like the fourth order term introduced for a single frequency in that it couples a ground state to the other ground state and back, but in this case that other state is a dressed state nearly resonant with the initial state due to the sideband. The denominator depends on the difference of the sideband frequency ω_s and the qubit frequency ω_q. This then gives us two levers with which to adjust this fourth order term's magnitude and sign: the intensity of the sideband and its frequency. We assume pure σ_+ polarization for all results regarding the bichromatic scheme.

In Table II we present the results of our search for doubly magic conditions with physically feasible parameters. As can be seen, doubly magic conditions exist for blue and red detuned traps and multiple pairs of states. Bringing the sideband frequency closer to the qubit frequency lowers the magic magnetic field, the trap depth and the residual sensitivity to the trapping light. Reducing the sideband intensity reduces the residual light sensitivity for a given magic trap depth and magnetic field. Lastly, the residual magnetic field sensitivity is entirely determined by the pairs of states chosen and even then is approximately the same for all pairs at the doubly magic point. Thus, bichromatic trapping light allows one to not only create a doubly magic trap but also to tune the parameters of the trap by adjusting the sideband strength and frequency.

We conclude by reiterating our results for doubly magic trapping conditions. Our analysis established that the fourth order Stark shift term is vital to differential Stark shift calculations at typical operating conditions and further explored the implications of the interaction of the laser and magnetic fields. With these tools we demonstrate light insensitive traps for a wide array of wavelengths, pairs of states, and bias magnetic fields. We then extended our analysis to a bichromatic trap with two optical frequencies separated by an amount similar to the splitting of the hyperfine ground states in Cesium. In doing so, we discovered doubly magic conditions in red and blue detuned traps for states separated by only one or two photons. These results provide a method for obtaining insensitivity to trapping lasers and magnetic field noise that could potentially improve atomic clock and quantum information experiments. Furthermore, we have relaxed many of the stringent requirements on wavelength, polarization, and states previously reported in the literature, making magic trapping more accessible to future experiments. We anticipate that similar results will be found for other alkali atom species.

This work was supported by NSF award PHY-1104531, the AFOSR Quantum Memories MURI, and the IARPA MQCO program through ARO contract W911NF-10-1-0347.

[1] M. Romalis and E. N. Fortson, Phys. Rev. A **59**, 4547 (1999).
[2] A. Negretti, P. Treutlein, and T. Calarco, Quantum Inf. Process. **10**, 721 (2011).
[3] J. M. Choi and D. Cho, J. Phys. Conf. Ser. **80**, 012037 (2007).
[4] V. Flambaum, V. A. Dzuba, and A. Derevianko, Phys. Rev. Lett. **101**, 220801 (2008).
[5] P. Rosenbusch, S. Ghezali, V. A. Dzuba, V. V. Flambaum, K. Beloy, and A. Derevianko, Phys. Rev. A **79**, 013404 (2009).
[6] H. Kim, H. S. Han, and D. Cho, Phys. Rev. Lett. **111**, 243004 (2013).
[7] N. Lundblad, M. Schlosser, and J. V. Porto, Phys. Rev. A **81**, 031611 (2010).
[8] Y. O. Dudin, R. Zhao, T. A. B. Kennedy, and A. Kuzmich, Phys. Rev. A **81**, 041805 (2010).
[9] A. Derevianko, Phys. Rev. A **81**, 051606(R) (2010).
[10] A. Derevianko, Phys. Rev. Lett. **105**, 033002 (2010).
[11] R. Chicireanu, K. D. Nelson, S. Olmschenk, N. Lundblad, A. Derevianko, and J. Porto, Phys. Rev. Lett. **106**, 063002 (2011).
[12] A. G. Radnaev, Y. O. Dudin, R. Zhao, H. H. Jen, S. D. Jenkins, A. Kuzmich, and T. A. B. Kennedy, Nat. Phys. **6**, 894 (2010).
[13] Supplementary material http...
[14] A. V. Taichenachev, V. I. Yudin, V. D. Ovsiannikov, and V. G. Pal'chikov, Phys. Rev. Lett. **97**, 173601 (2006).
[15] N. L. Manakov, V. D. Ovsiannikov, and L. P. Rapoport, Phys. Rep. **141**, 319 (1986).
[16] F. Le Kien, P. Schneeweiss, and A. Rauschenbeutel, Eur. Phys. J. D **67**, 1 (2013).
[17] E. Iskrenova-Tchoukova, M. S. Safronova, and U. I. Safronova, J. Comp. Meth. Sci. Eng. **7**, 521 (2007).
[18] S. Ulzega, A. Hofer, P. Moroshkin, and A. Weis, Europhys. Lett. **76**, 1074 (2006).
[19] S. Ulzega, A. Hofer, P. Moroshkin, and A. Weis, Europhys. Lett. **78**, 69901 (2007).
[20] A. Hofer, P. Moroshkin, S. Ulzega, and A. Weis, Phys. Rev. A **77**, 012502 (2008).
[21] E. Arimondo, M. Inguscio, and P. Violino, Rev. Mod. Phys. **49**, 31 (1977).
[22] A. Derevianko, M. S. Safronova, and W. R. Johnson, Phys. Rev. A **60**, R1741 (1999).
[23] B. Kaulakys, J . Phys. B: At. Mol. Opt. Phys. **28**, 4963 (1995).
[24] A. Kramida, Y. Ralchenko, J. Reader, and NIST ASD Team, http://physics.nist.gov/asd , version 5.1 (2013).
[25] J. E. Sansonetti, J. Phys. Chem. Ref. Data **38**, 761 (2009).
[26] W. Yei, A. Sieradzan, E. Cerasuolo, and M. D. Havey, Phys. Rev. A **57**, 3419 (1998).
[27] N. P. Georgiades, E. S. Polzik, and H. J. Kimble, Opt. Lett. **19**, 1474 (1994).

SUPPLEMENTARY INFORMATION FOR DOUBLY MAGIC TRAPPING FOR CS ATOM HYPERFINE CLOCK TRANSITIONS

In this supplementary material we provide details of the atomic calculations used to find magic conditions for monochromatic and bichromatic traps.

LIGHT - ATOM INTERACTION WITH ONE FREQUENCY OF LIGHT

We adopt an effective Hamiltonian approach between the ground states of Cesium. It is effective by virtue of the fact that no excited states explicitly appear in the Hamiltonian, instead our off-diagonal coupling terms account for the virtual processes through the excited states. We again write down an example Hamiltonian between $|0\rangle = |F = 3, M_F = 1\rangle$ and $|1\rangle = |F = 4, M_F = 1\rangle$ before delving into the computational specifics.

$$\mathcal{H} = \begin{pmatrix} V_{\mathrm{hf},0} + V_{00} + \beta_{00} + Z_{00} & V_{01} + \beta_{01} + Z_{01} \\ V_{01} + \beta_{01} + Z_{01} & V_{\mathrm{hf},1} + V_{11} + \beta_{11} + Z_{11} \end{pmatrix}$$

We have left the hyperfine interaction (HFI) as a perturbation term and thus all of the polarizability terms use fine structure energy denominators. For the second order polarizability we use the notation of [16]

$$V_{ij} = \frac{\Omega_0^2}{4} \sum_{\substack{K=0,1,2 \\ q=-K,..,K}} \alpha_{nJ}^{(K)} \{u^* \otimes u\}_{Kq} (-1)^{J+I+q-M_i+3F_i-M_j} \sqrt{2F_i+1} C_{F_i M_i K q}^{F_j M_j} \begin{Bmatrix} F_i & K & F_j \\ J & I & J \end{Bmatrix} \tag{5}$$

with the following further definitions for the reduced polarizability and polarization tensor

$$\alpha_{nJ}^{(K)} = (-1)^{K+J} \sqrt{2K+1} \sum_{n'J'} (-1)^{J'} \begin{Bmatrix} 1 & K & 1 \\ J & J' & J \end{Bmatrix} \left| \frac{\langle n'J' || r || nJ \rangle}{\langle 6p_{1/2} || r || 6s_{1/2} \rangle} \right|^2 \left(\frac{1}{\omega - \omega_{n'J'nJ}} + \frac{(-1)^{(K+1)}}{\omega + \omega_{n'J'nJ}} \right), \tag{6}$$

$$\{\mathbf{u}^* \otimes \mathbf{u}\}_{Kq} = \sum_{m,m'=0,\pm1} u^*_m u_{m'} C^{K,q}_{1,m,1,m'}\,, \tag{7}$$

with $K = 0, 1, 2$ a tensor rank corresponding to the scalar, vector and tensor polarizabilities, q a spherical tensor component, $\mathbf{u}$ a polarization vector written in the spherical tensor basis, I the nuclear spin and J, J' the total spin and orbital angular momentum of the ground and excited state, respectively. $\Omega_0 = \frac{\mathcal{E}}{\hbar}\langle 6p_{1/2}||er||6s_{1/2}\rangle$ is the reduced Rabi frequency with $\mathcal{E} = (2I_0/\epsilon_0 c)^{1/2}$, I_0 is the optical intensity and e is the elementary electric charge. As stated before $\omega_{n'J'nJ}$ is the energy difference between the ground state and an excited state without any hyperfine splitting, i.e. just fine structure energies. We write all of our results in terms of the reduced Rabi frequency, Ω_0. Finally, we only included four excited np states in our calculations $6p_{1/2}, 6p_{3/2}, 7p_{1/2}, 7p_{3/2}$. The reduced matrix elements from the $6s_{1/2}$ ground state to these states are given in Sec. . The static polarizability is dominated by the $6p$ terms, on the order of 96% according to [17], and the dynamic polarizabilities near these transitions are even more dominated by $6p$ since the energy denominators are even smaller for these states by roughly a factor of Δ/ω_{6s6p} with Δ the detuning from $6p$ while leaving relatively unchanged those of other states. The only other notable contribution is from $7p$, being the next allowed dipole transition, but as can be seen the reduced radial matrix element is an order of magnitude smaller along with carrying a much larger energy denominator for the cases we study.

Next is the hyperfine-mediated polarizability, β, that consists of two electric dipole couplings and a hyperfine interaction (HFI) coupling. This can be split into 4 broad categories based on the nature of the HFI matrix element: diagonal in the ground state, off-diagonal mixing of the ground state with other ns and nd levels, diagonal in the excited np levels, and off-diagonal mixing of excited np levels. We only account for those terms with a HFI diagonal in the ground states and those that mix the $6s$ ground state with excited ns states, as including other terms results in a smaller than 1% correction. More detailed discussion of the hyperfine-mediated polarizability can be found in [5], [18–20].

The term with the HFI matrix diagonal in the ground state term can be written as

$$\beta'_{ii} = -V_{\mathrm{hf},i} V'_{ii},$$

where $V'_{ii} = V_{ii}$ with the replacement $(\omega \pm \omega_{n'J'nJ}) \to (\omega \pm \omega_{n'J'nJ})^2$, and $V_{\mathrm{hf},i} = \langle 6s_{1/2} F_i M_i | V_{\mathrm{hf}} | 6s_{1/2} F_i M_i\rangle$ the diagonal matrix element of the standard magnetic dipole hyperfine operator[21] V_{hf} in the ground states.

The other term involving hyperfine mixing of the s ground state with excited ns states is a bit trickier. We approximate the hyperfine constant characterizing the mixing as [22]

$$A_{6sns} = \sqrt{A_{6s} A_{ns}}$$

which is verified empirically to work at the 1% level. The matrix element is related to this constant in the usual way

$$V_{\mathrm{hf,6sns}} = \langle 6s_{1/2} F M | V_{\mathrm{hf}} | ns_{1/2} F M\rangle = A_{6sns} \mathbf{I}\cdot\mathbf{J}$$

and the operator appearing in the Hamiltonian is

$$\beta''_{ij} = V_{\mathrm{hf,6sns}} V''_{ij}$$

with $V''_{ii} = V_{ii}$ where in one reduced matrix element the ground state is replaced by an excited s state,$\langle 6p_{1/2}||r||6s_{1/2}\rangle \to \langle 6p_{1/2}||r||ns_{1/2}\rangle$, and the energy denominator is now $(\omega \pm \omega_{n'J'nJ}) \to (\omega \pm \omega_{n'J'nJ})(\omega_{6s_{1/2},ns_{1/2}})$ and we include a sum over excited ns states. For this calculation we only include mixing up to $14s_{1/2}$ and use reduced electric dipole matrix elements calculated from a WKB approximation for elements involving $8s_{1/2}$ or higher. It is vital to note that the sign of the reduced matrix elements is now crucial since they are no longer squared in the polarizability, V''.

Combining the above contributions the hyperfine-mediated polarizability is

$$\beta_{ij} = \beta'_{ij}\delta_{i,j} + \beta''_{ij}$$

where the first term is diagonal and the second also contributes an off-diagonal vector component. We keep this vector component in our calculations though it is dwarfed by the second order vector polarizability by a factor that is approximately the hyperfine mixing matrix element divided by the energy difference between the ground state and an excited s state or $\simeq 10^{-5}$.

Two sources contribute the majority of the error in our calculation. First, the accuracy of our WKB approximation

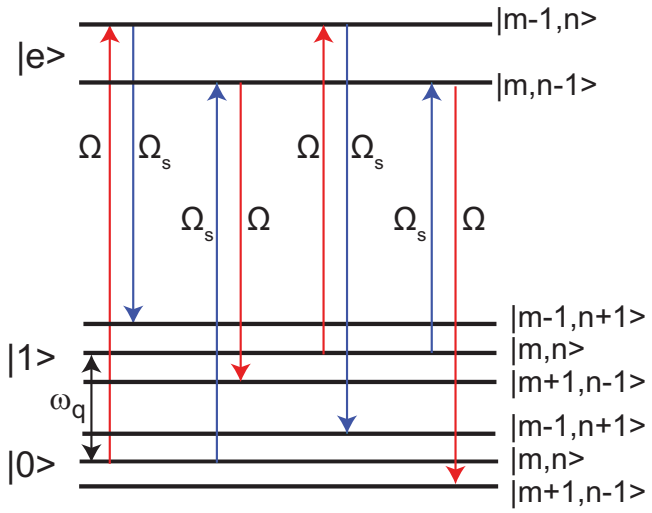

FIG. 3. The coupling for the bichromatic scheme with Ω representing coupling via the carrier laser and Ω_s that of the sideband. Four potential terms can contribute, but only two are important at any one time depending on sign of the sideband frequency ω_s. When $\omega_s \simeq \pm\omega_q$ two of the dressed states are becoming nearly degenerate with a dressed state of the other atomic ground state. This gives rise to a fourth order term that is tunable by the strength of the sideband and the sideband frequency.

of the reduced dipole matrix elements connecting $6p$ and $7p$ to excited ns levels is unknown. Secondly, β''_{ij} is known to converge slowly as a function of the included excited states and thus our truncation at $14s_{1/2}$ will introduce nontrivial inaccuracies. Comparison with recent experimental determinations of the DC Stark coefficient, k_s, yields an error of approximately 5%. A more pertinent test for our calculations is to compare against the experimental data in [5] for the differential light shift per unit of intensity. For 780 nm light they record $-2.27(40)\times10^{-2}\,\mathrm{Hz/W/cm^2}$ compared to our value of $-2.02\times10^{-2}\,\mathrm{Hz/W/cm^2}$ and for 532 nm light they measured $-3.51(70)\times10^{-4}\,\mathrm{Hz/W/cm^2}$ whereas we calculate $-4.08\times10^{-4}\,\mathrm{Hz/W/cm^2}$. Thus, in both cases we are within experimental error bars and differ by no more than 15%.

Finally there are Zeeman terms

$$Z_{ij} = \delta_{M_iM_j}\frac{\mu_B(-1)^{F_i+I+J+1}\sqrt{2F_i+1}}{\hbar} \times\left(g_J\sqrt{J(J+1)(2J+1)}\begin{Bmatrix} J & I & F_i\\ F_j & 1 & J\end{Bmatrix} + g_I(-1)^{F_j-F_i}\sqrt{I(I+1)(2I+1)}\begin{Bmatrix} I & J & F_i\\ F_j & 1 & I\end{Bmatrix}\right)C^{F_jM_j}_{F_iM_i10}.$$

Here we have specialized to the case of a static magnetic field polarized along $\hat{z}$. The diagonal coeffiients Z_{ii} give the usual expression for the hyperfine Zeeman shifts

$$Z_{ii} = \frac{M_i\mu_B g_{F_i}B}{\hbar}.$$

For the Cs ground state $g_J \simeq 2$, $g_{F=3} \simeq -1/4$, $g_{F=4} \simeq 1/4$, and the nuclear Landé factor is $g_I = -0.00039885395\,\mu_B = -0.73235679\,\mu_N$ with μ_B the Bohr magneton and μ_N the nuclear magneton.

BICHROMATIC LIGHT - ATOM INTERACTION

We now extend the above Hamiltonian to the two frequency case where we dress the ground states with sideband fields. The basis is $|0,m+1,n-1\rangle, |0,m,n\rangle, |0,m-1,n+1\rangle, |1,m+1,n-1\rangle, |1,m,n\rangle, |1,m-1,n+1\rangle$ where m and n are the photon numbers of the two fields with energy ω_m and ω_n, respectively, and $\omega_s = \omega_n - \omega_m$. The matrix dimension is then threefold larger than the monochromatic case as each ground state has two additional dressed states that differ in energy by $\pm\omega_s$ from the original state. In all other respects they are identical and the above definitions for matrix elements are still valid except that we must keep track of when the sideband amplitude is used.

To this end we introduce V^s when the sideband is one of the field amplitudes in the polarizability, $\Omega_0^2 \to \Omega_0\Omega_s$, and assume that when V_{ij} appears that one computes it for the carrier amplitude and the sideband amplitude, $\Omega_0^2 \to \Omega_s^2$ where Ω_s, is the reduced Rabi frequency for the sideband. Finally, for brevity we make the following substitution $\Delta E_i = V_{\mathrm{hf},i} + V_{ii} + \beta_{ii} + Z_{ii}$ and omit the vector contribution of the hyperfine-mediated polarizability, though again it is included in our full calculation. We write down a 6×6 example Hamiltonian for the ground states in the above basis with non-elliptical polarization for both fields.

$$\mathcal{H} = \begin{pmatrix} \Delta E_0 - \omega_s & V_{00}^s & 0 & Z_{01}+V_{01} & Z_{01}+V_{01}^s & 0 \\ V_{00}^s & \Delta E_0 & V_{00}^s & Z_{01}+V_{01}^s & Z_{01}+V_{01} & Z_{01}+V_{01}^s \\ 0 & V_{00}^s & \Delta E_0 + \omega_s & 0 & Z_{01}+V_{01}^s & Z_{01}+V_{01} \\ Z_{01}+V_{01} & Z_{01}+V_{01}^s & 0 & \Delta E_1 - \omega_s & V_{11}^s & 0 \\ Z_{01}+V_{01}^s & Z_{01}+V_{01} & Z_{01}+V_{01}^s & V_{11}^s & \Delta E_1 & V_{11}^s \\ 0 & Z_{01}+V_{01}^s & Z_{01}+V_{01} & 0 & V_{11}^s & \Delta E_1 + \omega_s \end{pmatrix}$$

At this point one can diagonalize and find the eigenvalues of the states $|0,m,n\rangle$ and $|1,m,n\rangle$ to acquire the shifts of the atomic state due to the magnetic and A.C. electric fields.

NUMERICAL VALUES

In this section we list the hyperfine constants and radial reduced matrix elements used for calculations. Table I gives hyperfine constants and Tables II-V give radial matrix elements. Where possible we have used numerical values from [17]. For other transitions we have used the values found from WKB calculations following the theory of Ref. [23]. As a check on the WKB calculations we compare them in the tables to the published values in [17] and to Coulomb wave function (Cwf) calculations. The WKB and Cwf calculations use effective quantum defects extracted from the energy values listed in [24, 25]. We estimate the error of the WKB matrix elements to be less than 10% on the basis of comparison to values from [17]. The Cwf and WKB calculations give a value for $R_{nl_j}^{nl'_{j'}}$ which is converted to a reduced matrix element using

$$\langle n'l'sj'||r||nlsj\rangle = (-1)^{1+s+j+(1+l+l')/2}\sqrt{(2j+1)(2j'+1)\max(l,l')}\begin{Bmatrix} l & s & j \\ j' & 1 & l' \end{Bmatrix} R_{nl_j}^{n'l'_{j'}}.$$

When calculating the third order hf-Stark polarizability the sign of the reduced matrix elements is significant. Note that $\langle n'j'||T||nj\rangle = (-1)^{j-j'}\langle nj||T||n'j'\rangle$. Thus $\langle n'p_{1/2}||T||ns_{1/2}\rangle = \langle ns_{1/2}||T||n'p_{1/2}\rangle$ but $\langle n'p_{3/2}||T||ns_{1/2}\rangle = -\langle ns_{1/2}||T||n'p_{3/2}\rangle$. There is inconsistency in the literature as regards signs of published reduced matrix elements. We have taken the signs from our Cwf or WKB calculations which agree with each other.

This work was supported by NSF award PHY-1104531, the AFOSR Quantum Memories MURI, and the IARPA MQCO program through ARO contract W911NF-10-1-0347.

state	A (MHz)	B (MHz)
$6s_{1/2}$	2298.1579425	
$7s_{1/2}$	546.3	
$8s_{1/2}$	218.9	
$9s_{1/2}$	110.1	
$10s_{1/2}$	63.2	
$11s_{1/2}$	39.4	
$12s_{1/2}$	26.31	
$13s_{1/2}$	18.40	
$14s_{1/2}$	13.41	
$15s_{1/2}$	10.1^c	
$6p_{1/2}$	291.9309^c	
$7p_{1/2}$	94.35	
$8p_{1/2}$	42.97	
$9p_{1/2}$	23.19	
$6p_{3/2}$	50.28825^c	-0.4940^c
$7p_{3/2}$	16.605	-0.15
$8p_{3/2}$	7.58	-0.14
$9p_{3/2}$	4.123	-0.051
$5d_{3/2}$	48.78^a	0.1^a
$6d_{3/2}$	16.34^c	-0.1^c
$7d_{3/2}$	7.4^c	
$8d_{3/2}$	3.95^c	
$5d_{5/2}$	-21.24^a	0.2^a
$6d_{5/2}$	-4.69^b	0.18^b
$7d_{5/2}$	-1.7	
$8d_{5/2}$	-0.85	

TABLE III. Some hyperfine constants of Cs. Values from [21] except for a) Ref. [26], b) Ref. [27], c) Ref. [25]

.

final state	transition wavelength (μm)	theory $\langle nl_j\|\|r\|\|6p_{1/2}\rangle^a$	$r_{\rm min}$	Cwf $\langle nl_j\|\|r\|\|6p_{1/2}\rangle$	WKB $\langle nl_j\|\|r\|\|6p_{1/2}\rangle$
$6s_{1/2}$	-0.8946	4.489	0.	4.501	4.482
$7s_{1/2}$	1.359	−4.236	0.	-3.921	-3.970
$8s_{1/2}$	0.7611		0.	-0.9379	-0.9650
$9s_{1/2}$	0.6356		0.	-0.4956	-0.5159
$10s_{1/2}$	0.5840		0.	-0.3270	-0.3434
$11s_{1/2}$	0.5570		0.	-0.2396	-0.2533
$12s_{1/2}$	0.5408		0.	-0.1867	-0.1983
$13s_{1/2}$	0.5303		0.	-0.1513	-0.1614
$14s_{1/2}$	0.5230		0.	-0.1262	-0.1351
$15s_{1/2}$	0.5178		0.	-0.1075	-0.1155
$5d_{3/2}$	3.011	7.06	0.7	7.317	7.056
$6d_{3/2}$	0.8764	-4.15	0.7	-4.002	-4.228
$7d_{3/2}$	0.6725		0.7	-1.976	-2.070
$8d_{3/2}$	0.6012		0.7	-1.256	-1.308

TABLE IV. Reduced matrix elements of coupled states $|nlsj\rangle$ in the j basis $\langle n'l'sj'||r||6p_{1/2}\rangle$ for the Cs $6p_{1/2}$ state and transition vacuum wavelengths. Cwf are values calculated using Coulomb wavefunctions with experimental values for quantum defects, and $r_{\rm min}$ a small r cutoff to avoid divergence. WKB are values calculated using the theory of [23]. Matrix elements are given in atomic units. a)From [17] with the sign from Cwf calculation.

final state	transition wavelength (μm)	theory $\langle nl_j\|\|r\|\|6p_{3/2}\rangle^a$	$r_{\rm min}$	Cwf $\langle nl_j\|\|r\|\|6p_{3/2}\rangle$	WKB $\langle nl_j\|\|r\|\|6p_{3/2}\rangle$
$6s_{1/2}$	-0.8523	6.324	0.	6.309	6.2856
$7s_{1/2}$	1.470	−6.473	0.	-6.026	-6.0946
$8s_{1/2}$	0.7946		0.	-1.349	-1.3847
$9s_{1/2}$	0.6588		0.	-0.7049	-0.7318
$10s_{1/2}$	0.6036		0	-0.4632	-0.4848
$11s_{1/2}$	0.5747		0.	-0.3386	-0.3568
$12s_{1/2}$	0.5575		0.	-0.2634	-0.2789
$13s_{1/2}$	0.5463		0.	-0.2134	-0.2269
$14s_{1/2}$	0.5386		0.	-0.1779	-0.1898
$15s_{1/2}$	0.5331		0.	-0.1515	-0.1621
$5d_{3/2}$	3.614	−3.19	0.7	-3.259	-3.167
$5d_{5/2}$	3.491	9.66	0.7	9.871	9.594
$6d_{3/2}$	0.9211	2.05	0.7	2.003	2.0923
$6d_{5/2}$	0.9175	−6.01	0.7	-5.860	-6.129
$7d_{3/2}$	0.6985		0.7	0.9524	0.9857
$7d_{5/2}$	0.6975		0.7	-2.816	-2.919
$8d_{3/2}$	0.6220		0.7	0.5973	0.6142
$8d_{5/2}$	0.6215		0.7	-1.773	-1.827

TABLE V. Reduced matrix elements of coupled states $|nlsj\rangle$ in the j basis $\langle n'l'sj'||r||6p_{3/2}\rangle$ for the Cs $6p_{3/2}$ state and transition vacuum wavelengths. Cwf are values calculated using Coulomb wavefunctions with experimental values for quantum defects, and $r_{\rm min}$ a small r cutoff to avoid divergence. WKB are values calculated using the theory of [23]. Matrix elements are given in atomic units. a)From [17] with the sign from Cwf calculation.

final state	transition wavelength (μm)	theory $\langle nl_j\|\|r\|\|7p_{1/2}\rangle^a$	$r_{\min}$	Cwf $\langle nl_j\|\|r\|\|7p_{1/2}\rangle$	WKB $\langle nl_j\|\|r\|\|7p_{1/2}\rangle$
$6s_{1/2}$	-0.4594	0.276	0.	0.465	0.4175
$7s_{1/2}$	-3.096	10.308	0.	10.18	10.18
$8s_{1/2}$	3.919	-9.313	0.	-9.115	-9.154
$9s_{1/2}$	1.943		0.	-1.921	-1.940
$10s_{1/2}$	1.530		0.	-0.9761	-0.9909
$11s_{1/2}$	1.358		0.	-0.6338	-0.6460
$12s_{1/2}$	1.265		0.	-0.4612	-0.4716
$13s_{1/2}$	1.209		0.	-0.3583	-0.3674
$14s_{1/2}$	1.172		0.	-0.2904	-0.2985
$15s_{1/2}$	1.146		0.	-0.2424	-0.2497
$5d_{3/2}$	-1.376		0.7	-1.897	-2.091
$6d_{3/2}$	12.14	18.0	0.7	17.92	17.86
$7d_{3/2}$	2.335	6.56	0.7	-6.402	-6.519
$8d_{3/2}$	1.654		0.7	-3.124	-3.193

TABLE VI. Reduced matrix elements of coupled states $|nlsj\rangle$ in the j basis $\langle n'l'sj'||r||7p_{1/2}\rangle$ for the Cs $7p_{1/2}$ state and transition vacuum wavelengths. Cwf are values calculated using Coulomb wavefunctions with experimental values for quantum defects, and $r_{\min}$ a small r cutoff to avoid divergence. WKB are values calculated using the theory of [23]. Matrix elements are given in atomic units. a)From [17] with the sign from Cwf calculation.

final state	transition wavelength (μm)	theory $\langle nl_j\|\|r\|\|7p_{3/2}\rangle^a$	$r_{\min}$	Cwf $\langle nl_j\|\|r\|\|7p_{3/2}\rangle$	WKB $\langle nl_j\|\|r\|\|7p_{3/2}\rangle$
$6s_{1/2}$	-0.4557	0.586	0.	0.8158	0.7534
$7s_{1/2}$	-2.932	14.320	0.	14.13	14.13
$8s_{1/2}$	4.218		0.	-13.78	-13.84
$9s_{1/2}$	2.014		0.	-2.681	-2.705
$10s_{1/2}$	1.574		0.	-1.343	-1.361
$11s_{1/2}$	1.392		0.	-0.8672	-0.8825
$12s_{1/2}$	1.295		0.	-0.6294	-0.6424
$13s_{1/2}$	1.236		0.	-0.4882	-0.4996
$14s_{1/2}$	1.197		0.	-0.3953	-0.4054
$15s_{1/2}$	1.170		0.	-0.3298	-0.3389
$5d_{3/2}$	-1.343		0.7	0.7573	0.8310
$5d_{5/2}$	-1.361		0.7	-2.369	-2.591
$6d_{3/2}$	15.57	-8.07	0.7	-8.029	-8.011
$6d_{5/2}$	14.59	24.4	0.7	24.22	24.16
$7d_{3/2}$	2.438	3.32	0.7	3.253	3.300
$7d_{5/2}$	2.426	-9.64	0.7	-9.459	-9.604
$8d_{3/2}$	1.705		0.7	1.520	1.546
$8d_{5/2}$	1.702		0.7	-4.473	-4.554

TABLE VII. Reduced matrix elements of coupled states $|nlsj\rangle$ in the j basis $\langle n'l'sj'||r||7p_{3/2}\rangle$ for the Cs $7p_{3/2}$ state and transition vacuum wavelengths. Cwf are values calculated using Coulomb wavefunctions with experimental values for quantum defects, and $r_{\min}$ a small r cutoff to avoid divergence. WKB are values calculated using the theory of [23]. Matrix elements are given in atomic units. a)From [17] with the sign from Cwf calculation.